

# Direct Conversion of Fibroblasts to Neurons by Reprogramming PTB-Regulated MicroRNA Circuits

Yuanchao Xue,<sup>1,2</sup> Kunfu Ouyang,<sup>3</sup> Jie Huang,<sup>1</sup> Yu Zhou,<sup>1,2</sup> Hong Ouyang,<sup>4</sup> Hairi Li,<sup>2</sup> Gang Wang,<sup>3</sup> Qijia Wu,<sup>1</sup> Chaoliang Wei,<sup>2</sup> Yanzhen Bi,<sup>1</sup> Li Jiang,<sup>1</sup> Zhiqiang Cai,<sup>1</sup> Hui Sun,<sup>1</sup> Kang Zhang,<sup>4</sup> Yi Zhang,<sup>1,5</sup> Ju Chen,<sup>3</sup> and Xiang-Dong Fu<sup>1,2,4,\*</sup>

<sup>1</sup>State Key Laboratory of Virology, College of Life Sciences, Wuhan University, Wuhan, Hubei 430072, China

<sup>2</sup>Department of Cellular and Molecular Medicine

<sup>3</sup>Department of Medicine

<sup>4</sup>Institute of Genomic Medicine

University of California, San Diego, La Jolla, CA 92093-0651, USA

<sup>5</sup>Present address: Center for Genome Analysis, ABLife Inc., Novonest Building 214, 8 Nanhu Avenue, East Lake Hi-Tech Development Zone, Wuhan, Hubei 430079, China

\*Correspondence: xdfu@ucsd.edu

<http://dx.doi.org/10.1016/j.cell.2012.11.045>

## SUMMARY

The induction of pluripotency or *trans*-differentiation of one cell type to another can be accomplished with cell-lineage-specific transcription factors. Here, we report that repression of a single RNA binding polypyrimidine-tract-binding (PTB) protein, which occurs during normal brain development via the action of miR-124, is sufficient to induce *trans*-differentiation of fibroblasts into functional neurons. Besides its traditional role in regulated splicing, we show that PTB has a previously undocumented function in the regulation of microRNA functions, suppressing or enhancing microRNA targeting by competitive binding on target mRNA or altering local RNA secondary structure. A key event during neuronal induction is the relief of PTB-mediated blockage of microRNA action on multiple components of the REST complex, thereby derepressing a large array of neuronal genes, including miR-124 and multiple neuronal-specific transcription factors, in nonneuronal cells. This converts a negative feedback loop to a positive one to elicit cellular reprogramming to the neuronal lineage.

## INTRODUCTION

Feedback and feedforward circuits are key regulatory strategies for maintaining gene expression programs in specific cell types, and factors that alter the homeostatic balance of these circuits can induce enduring program switches in cell differentiation and development (Zernicka-Goetz et al., 2009). Many regulatory pathways use such mechanisms to control the output of biological responses through gene networks in transcription (Amit

et al., 2009), RNA metabolism (Coutinho-Mansfield et al., 2007; Lareau et al., 2007), signal transduction (Carracedo and Pandolfi, 2008), and macromolecular synthesis and degradation (Auld and Silver, 2006).

MicroRNAs have emerged as key mediators in various modes of feedback and feedforward regulation (Leung and Sharp, 2010). MicroRNA are expressed in all higher eukaryotes, ~800 in humans, and a recent estimate suggests that up to 60% of human genes may be subjected to microRNA control (Bartel, 2009). In many cases, homeostasis is achieved by feedback controls in which specific transcription factors or RNA-binding proteins regulate the expression and biogenesis of microRNAs, which, in turn, suppress the expression of their regulators.

Neuronal differentiation is a well-studied paradigm as a consequence of transcription reprogramming (Li and Jin, 2010). Recent studies show that a set of neuronal-specific transcription factors is sufficient to *trans*-differentiate fibroblasts into functional neurons (Caiazza et al., 2011; Kim et al., 2011; Pang et al., 2011; Qiang et al., 2011; Vierbuchen et al., 2010; Yang et al., 2011). Several neuronal-specific microRNA, such as miR-9/9\* and miR-124, also play key roles in this process (Yoo et al., 2011). miR-124 is a well-known regulator of the transcription silencing complex built on RE1-silencing transcription factor (REST), which represses a large array of neuronal-specific genes in nonneuronal cells; this includes miR-124 itself, thus forming an autoregulatory loop during neuronal differentiation (Ballas et al., 2005; Conaco et al., 2006). Forced expression of miR-124 can drive differentiation of neural progenitor cells to neurons (Cheng et al., 2009) and C2C12 cells to become neuronal-like cells (Watanabe et al., 2004).

Regulated RNA processing also plays a critical role in neuronal differentiation. The polypyrimidine-tract-binding (PTB) protein and its homolog nPTB undergo a programmed switch during neuronal differentiation (Boutz et al., 2007; Makeyev et al., 2007; Zheng et al., 2012). miR-124 is able to modulate such switch by reducing PTB, thereby reprogramming an array of

neuronal-specific alternative splicing events, and forced expression of PTB is able to block miR-124-induced neuronal differentiation (Makeyev et al., 2007). However, it has been unclear whether the PTB/nPTB switch is sufficient to initiate neuronal differentiation, and if so, which specific PTB/nPTB-regulated splicing events contribute to such cell fate switch.

We previously reported global PTB-RNA interactions in the human genome (Xue et al., 2009). In PTB-depleted cells, we unexpectedly observed conversion of diverse cell types into neuronal-like cells. In addition to induced alternative splicing events, we found an extensive involvement of PTB in the regulation of microRNA targeting through either direct competition or induced switch of local RNA secondary structure. A key event is the activation of the miR-124/REST loop in which PTB not only serves as a target, but also acts as a potent regulator. Consequently, regulated PTB expression induces massive reprogramming at both the splicing and microRNA levels to drive the cell fate decision toward the neuronal lineage.

## RESULTS

### PTB Downregulation Switches Multiple Cell Types to Neuronal-like Cells

We attempted to use specific small hairpin RNAs (*shRNAs*) to stably knock down PTB in order to systematically analyze PTB-regulated splicing. As expected, *shPTB* induced nPTB expression in HeLa cells (Figure S1A available online). We noted a slow-growth phenotype of *shPTB*-treated cells, which was also seen by others (He et al., 2007). Strikingly, many PTB-depleted HeLa cells exhibited neurite outgrowth, and further analysis revealed the expression of several neuron markers, including class III  $\beta$ -tubulin (known as Tuj1) and MAP2 (Figures 1A and S1A), suggesting that PTB knockdown converted highly transformed HeLa cells to neuronal-like cells.

We extended this analysis to multiple cell types of diverse origin, including human embryonic carcinoma stem cells (NT2), mouse neural progenitor cells (N2A), human retinal epithelial cells (ARPE19), and primary mouse embryonic fibroblasts (MEFs). Upon PTB knockdown (Figure S1B), all of these cells exhibited a neuronal-like morphology and showed strong Tuj1 staining (Figure 1A). Neuronal committed N2A and NT2 cells were potentially induced to show typical neuronal morphology in  $\sim$ 5 days after PTB knockdown and develop more complex morphology after the cells were switched to N3 media containing a set of neural growth factors for 3–5 days. ARPE19 and MEFs took  $\sim$ 2 weeks to develop typical neuronal morphology in N3 media. Control *shRNA* treatment had no effect under these conditions.

We further characterized two of these cell lines (N2A and MEFs) by examining additional neural markers, including Synapsin 1 (SYN1), vGLUT1, and NeuN (Figure 1B). SYN1 and vGLUT1 showed a typical punctate staining pattern on Tuj1-positive cells, but not on undifferentiated cells in the same field (Figure 1B). We also detected strong staining of GABA channel receptors on these derived neurons (data not shown). As previously described (Vierbuchen et al., 2010), immunostaining and RT-PCR analyses ruled out potential contamination of our starting MEFs with neural crest cells (Figures S1C and S1D).

Both N2A cells and MEFs were efficiently converted by two distinct *shRNAs* against PTB to neuronal-like cells (Figure S1E). Importantly, the effect of specific *shPTB* molecules could each be rescued with the *shRNA*-resistant PTB expression unit that carries synonymous mutations (M1 or M2) in their targeting sites, thus ruling out potential off-target effects (Figure 1C). Time-course analysis demonstrated that PTB knockdown progressively converted MEFs to neuronal-like cells with complex morphology (Figures 1D and 1E). These data strongly suggest that PTB downregulation potentially induced these cells to differentiate (in the case of N2A cells) or *trans*-differentiate (in the case of MEFs) into neurons.

### MEF-Derived Neurons Are Functional with Synaptic Activities

To determine the functionality of differentiated cells, we patch-clamped both *shPTB*-induced neurons from N2A cells and MEFs. We observed that 11 out of 12 N2A cell-derived neurons exhibited fast inward  $\text{Na}^+$  currents and action potential upon membrane depolarization (Figure S2A) and that seven out of eight *shPTB*-induced MEFs showed a similar response, which could be blocked by tetrodotoxin (TTX), a specific inhibitor of sodium channels (Figure 2A). Both of these induced cell types showed depolarization-induced  $\text{Ca}^{2+}$  influx (Figures S2B and S2C). We next determined whether MEF-derived neurons are fully functional in the presence of primary astrocytes, which is known to be essential for *trans*-differentiated MEFs to become synaptically competent (Vierbuchen et al., 2010). After coculture for a week with freshly isolated astrocytes free of contaminating neurons from the brain of a green fluorescent protein (GFP)-transgenic rat, we detected repetitive action potentials of varying frequencies driven by current pulse in five out of six MEFs-derived neurons (Figure 2B). Importantly, we recorded synaptic activities on six out of seven such neurons examined (Figures 2C and 2D).

The detected postsynaptic currents likely reflect both glutamatergic and GABAergic responses, because 6-cyano-7-nitroquinoxaline-2,3-dione (CNQX) plus D(-)-2-amino-5-phosphonovaleric acid (APV) (antagonists of glutamatergic channel receptors) and Picrotoxin (PiTX, antagonist of GABA<sub>A</sub> channel receptors) could sequentially block the expected signals (Figures 2E and 2F). We further recorded GABA-induced, PiTX-sensitive currents upon focal application of GABA (Figure 2G). In the presence of PiTX, we detected AMPA-receptor-mediated excitatory postsynaptic currents (EPSCs) with fast kinetics when holding the neuron at  $-70\text{mV}$  with an external solution containing  $2\text{ mM Mg}^{2+}$  (Figure 2H), which is known to inhibit N-methyl-D-aspartate (NMDA) EPSC with slow kinetics (Nowak et al., 1984). By holding the neuron at  $+60\text{mV}$  to relieve the inhibitory effect of  $\text{Mg}^{2+}$ , we detected both NMDA and AMPA EPSCs, which could be progressively blocked by the NMDA channel inhibitor APV and the AMPA channel antagonist CNQX (Figure 2H). These data demonstrated that *shPTB* had *trans*-differentiated MEFs into functional neurons.

### PTB Regulates the Expression of Many Neuronal Genes in Nonneuronal Cells

Because of the induced neuronal morphology and the availability of the genome-wide PTB-RNA interaction map on HeLa cells

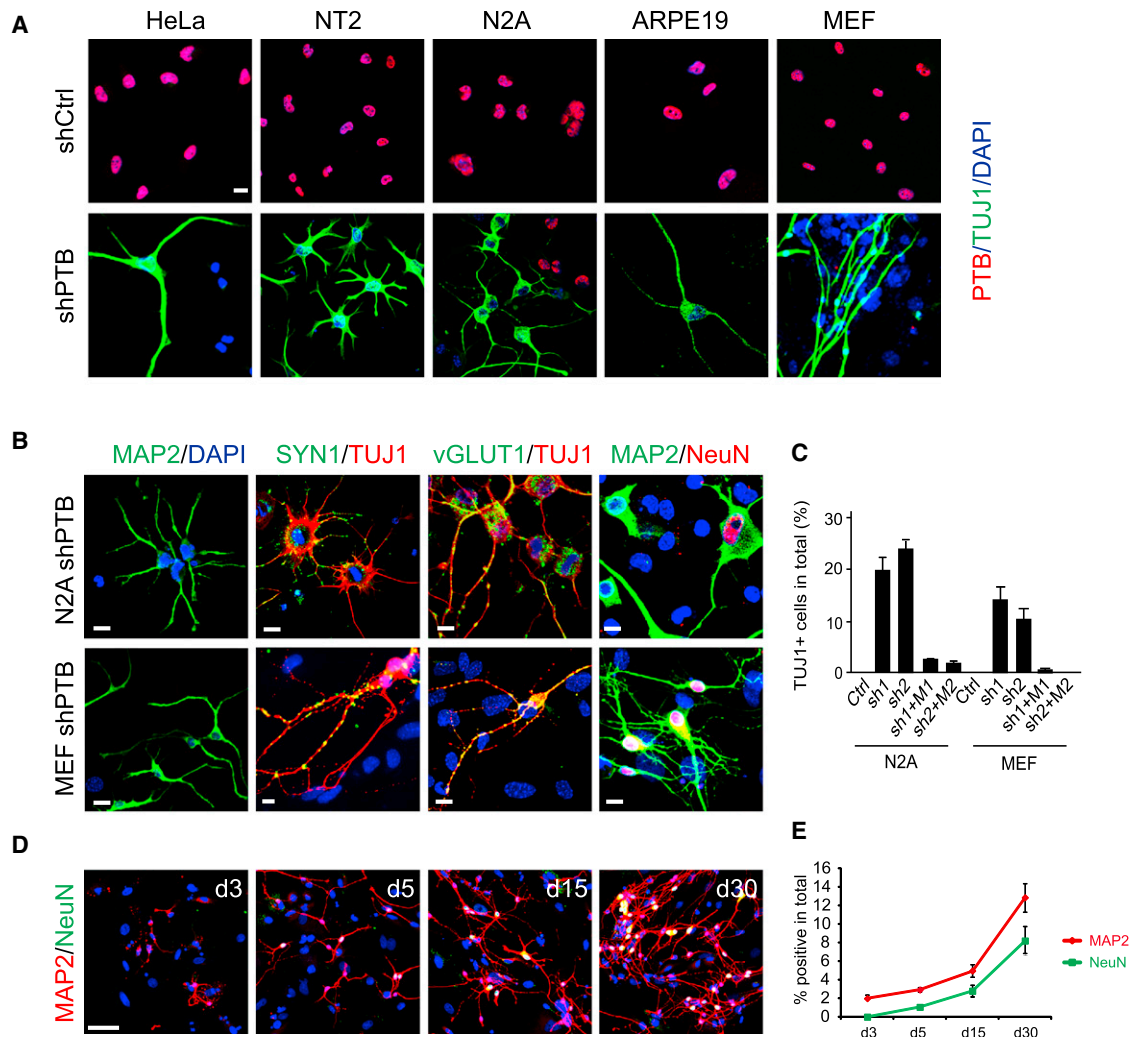


**Figure 1. Differentiation of Diverse Cell Types into Neuronal-like Cells in Response to PTB Knockdown**

(A) Induction of neuronal morphology and the expression of the neuronal marker TuJ1 in multiple cell types in response to depletion of PTB. Scale bar, 20  $\mu$ m.

(B) Characterization of two cell types (N2A and MEF) with additional neural markers. Typical punctate staining is evident (yellow) with antibodies against Synapsin and vGLUT1. Scale bar, 20  $\mu$ m.

(C) Quantification of induced neuronal-like cells derived from N2A and MEFs. The data were based on positive TuJ1-stained cells divided by initial plating cells in response to two separate *shPTBs* (sh1 and sh2). The effect could be efficiently rescued with the corresponding *shRNA*-resistant PTB expression units that contain mutations in the corresponding target sites (M1 and M2). Data are shown as mean  $\pm$  SD.

(D) Time course analysis of neuronal induction on *shPTB*-treated MEFs after switching to N3 media. MAP2 and NeuN were stained at indicated time points. Scale bar, 60  $\mu$ m.

(E) Quantified temporal profile of PTB knockdown-induced neurons. Data shown as mean  $\pm$  SD are based on four equivalent areas shown in (D).

See also Figure S1.

(Xue et al., 2009), we initially took this cell type as a surrogate model to understand *shPTB*-induced cellular reprogramming. We identified by RNA-seq a large number of up- or downregulated genes induced by *shPTB* (Figure S3A), and we further confirmed a panel of these events by quantitative RT-PCR (qRT-PCR) (Figure S3B). Gene ontology analysis showed that many such altered genes were linked to neuronal functions (Figure S3C). These observations indicate that PTB is extensively involved in the regulation of neuronal genes in nonneuronal cells.

We noted the induction of *Brn2* and *Myt1l*, which correspond to two out of five key transcription factors previously shown to be sufficient to induce *trans*-differentiation of fibroblasts into neurons (Vierbuchen et al., 2010). Because HeLa cells have a severely rearranged genome, we performed a focused analysis on MEFs by qRT-PCR (Figure 3A), detecting the induction of all five critical transcription factors (*Ascl1*, *Brn2*, *Myt1l*, *Zic1*, and *Olig2*) as well as *NeuroD1* known to enhance neurogenesis in human fibroblasts (Pang et al., 2011). We also observed the induction of miR-124 and miR-9 (Figure 3A), which have been

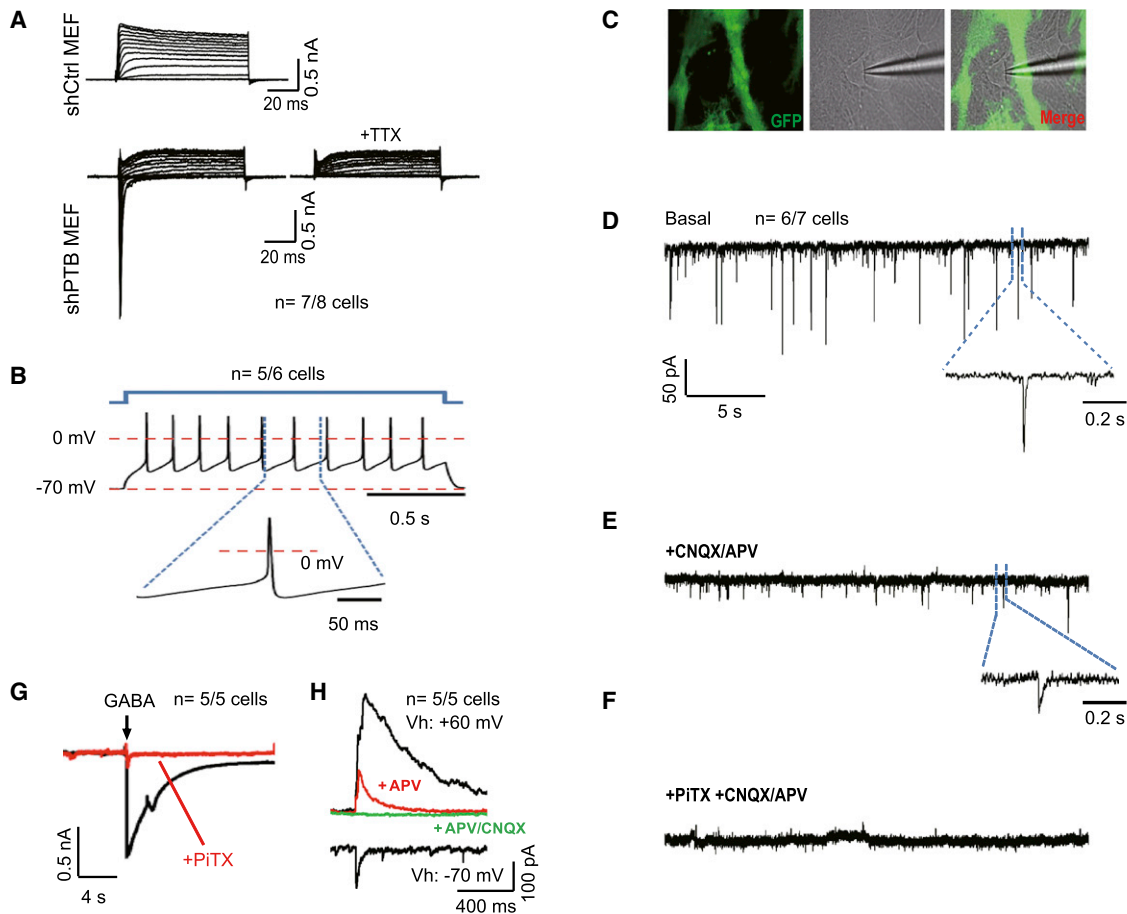


**Figure 2. Synaptic Activities on Neurons Derived from *shPTB*-Induced MEFs**

(A) Representative traces of whole-cell currents on control *shRNA*-treated (top) and *shPTB*-treated (bottom) MEFs. Only *shPTB*-treated MEFs exhibited fast inward sodium currents, which could be blocked by 1  $\mu$ M sodium channel inhibitor TTX.

(B) Representative trace of action potentials in response to step current injections on *shPTB*-induced neurons after coculturing with rat glial cells.

(C) Image of an *shPTB*-induced neuron cocultured with GFP-marked rat glial cells. Recording electrode was patched on the *shPTB*-induced neuron (middle and right).

(D–F) Representative traces of spontaneous postsynaptic currents on *shPTB*-induced neurons (D). The cell was held at  $-70$  mV, revealing events of various amplitudes and frequencies. The inset shows a representative trace of synaptic response. Glutamatergic synaptic currents were blocked with 20  $\mu$ M CNQX plus 50  $\mu$ M APV (E). The inset highlights the remaining GABA current. GABA currents were blocked with 50  $\mu$ M PITX (F).

(G) Induction of GABA currents by focal application of 1 mM GABA, which could be blocked by PITX (red).

(H) Representative trace of synaptic currents recorded on *shPTB*-induced neurons. Vh: holding potential. AMPA-R-mediated EPSC was recorded at  $-70$  mV. Blockage of  $Mg^{2+}$  to NMDA-R was relieved at  $+60$  mV, revealing both AMPA and NMDA EPSCs, which could be sequentially blocked with 50  $\mu$ M APV (antagonist of NMDA-type glutamate receptors) and 20  $\mu$ M CNQX (antagonist of AMPA receptors).

The number of cells that show the representative response against total cells examined is indicated in each panel. See also Figure S2.

shown to synergize with neuronal-specific transcription factors in promoting neurogenesis (Yoo et al., 2011). These data explain the compatible functionality of *shPTB*-induced neurons to that converted by a set of lineage-specific transcription factors.

### REST Activity Contributes a Key Part to the *shPTB*-Induced Neuronal Program

The REST complex is known to repress a large set of neuronal genes in nonneuronal cells (Johnson et al., 2007). Interestingly, we noted that all induced transcription factors examined in Figure 3A contain significant REST ChIP-seq signals from the ENCODE data on C2C12 cells. We confirmed strong REST

binding by ChIP-qPCR on most of these genes in MEFs, and, as expected, REST knockdown induced the expression of these genes (Figures S3D and S3E). These data suggest that the function of the REST complex might be compromised in *shPTB*-treated MEFs.

To determine how the REST complex was compromised, we examined the response of REST and REST cofactors to *shPTB* in HeLa cells. While REST expression was little affected from our RNA-seq analysis, we found that *SCP1*, a Pol II Ser5 phosphatase associated with the REST complex (Yeo et al., 2005), was significantly downregulated by *shPTB* in multiple cell types with induced neuronal morphology (Figure 3B). The effect of

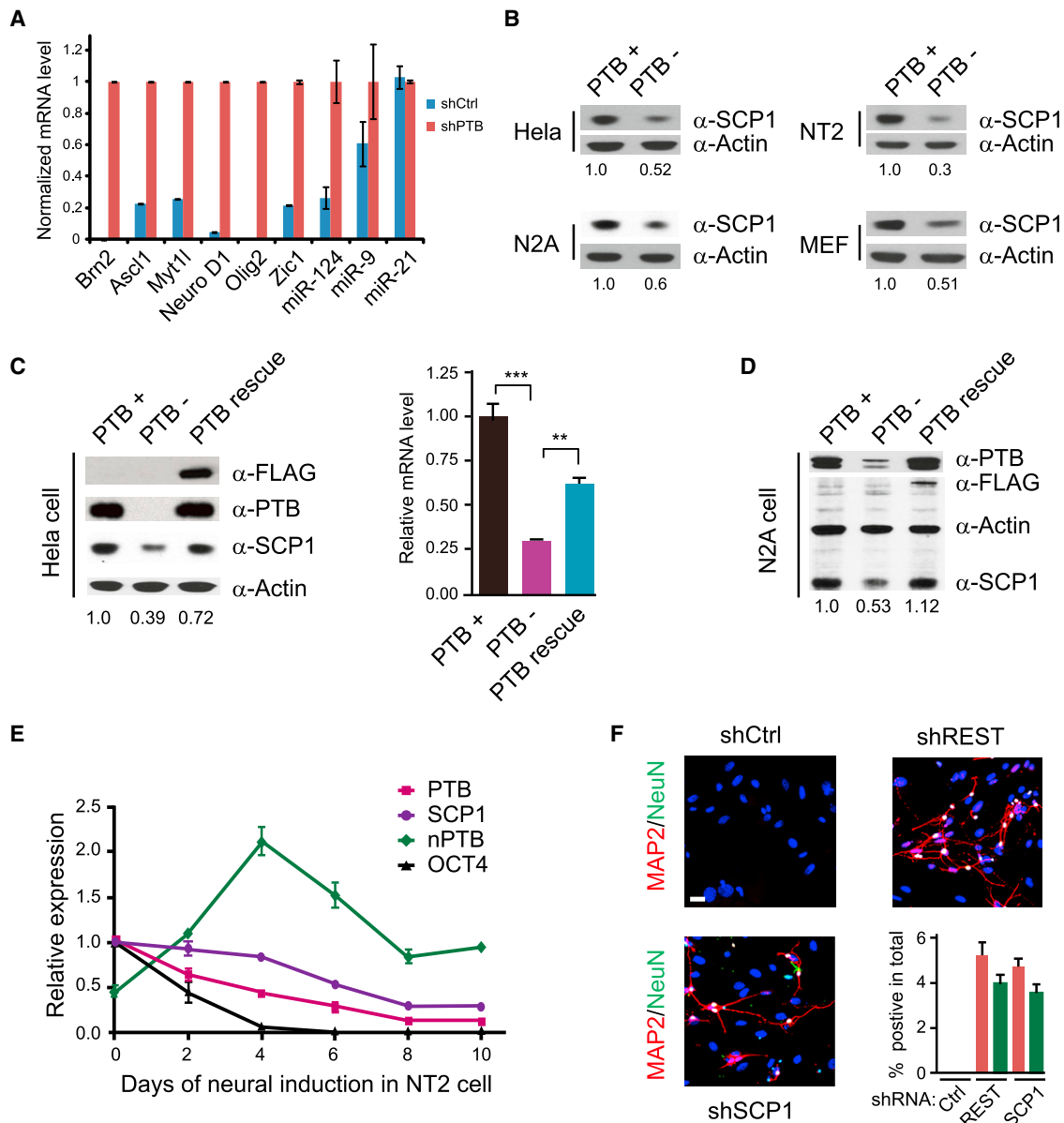


**Figure 3. Derepression of Neuronal-Specific Genes in Response to PTB Knockdown**

(A) qRT-PCR analysis of a panel of transcription factors and microRNAs in *shPTB*-treated MEFs. Data are normalized against Actin; miR-21 served as a negative control.

(B) Downregulation of SCP1 in multiple cell types determined by western blotting.

(C and D) Rescue of SCP1 expression in PTB knockdown cells by an *shRNA*-resistant PTB in HeLa (C) and N2A (D) cells.

(E) Time-course analysis of neural induction by retinoic acid (RA) on NT2 cells analyzed by qRT-PCR. *Oct4* was analyzed as a control. Data are shown as mean  $\pm$  SD.

(F) Induction of neuronal differentiation on MEFs with *shRNA* against *SCP1* or *REST*. The induction efficiency was calculated based on the number of cells with positive MAP2 and NeuN staining divided by total plating cells.

Data are shown as mean  $\pm$  SD. See also Figure S3.

*shPTB* on *SCP1* expression could be rescued on two of these cell types we examined (Figures 3C and 3D). During the course of retinoic-acid-induced neural differentiation on NT2 cells, we observed that *SCP1* expression was gradually reduced, which closely tracked PTB downregulation and nPTB induction (Fig-

ure 3E). These findings suggest that PTB-regulated expression of the REST cofactor SCP1 may play a key role in neuronal differentiation under physiological conditions.

Recent studies suggest that REST is required for maintaining the population of neural stem cells (Gao et al., 2011) and genetic

inactivation of REST does not efficiently turn fibroblasts into neurons, despite the induction of some neuronal genes (Aoki et al., 2012). However, a dominant-negative *SCP1* was able to efficiently drive neuronal differentiation on P19 cells (Yeo et al., 2005). We thus wished to directly test the contribution of *SCP1* to *shPTB*-induced neurogenesis under our experimental conditions, and we similarly tested REST for comparison. We found that both *shSCP1* and *shREST*, but not control *shRNA*, were able to trigger neuronal differentiation on MEFs (Figure 3F). The neural induction efficiency by *shSCP1* and *shREST* was similar, but lower than that induced by *shPTB* (compared Figure 1C and Figure 3F), indicating that other PTB-regulated events may additionally contribute to the induction of neurogenesis. The reason for efficient induction of neurogenesis with *shPTB* or *shRNA* against *REST* or a REST cofactor gene may be due to gradual switch of these cell-lineage-specific regulators, which may mimic relevant developmental processes (see Discussion).

### PTB-Regulated Splicing Likely Facilitates the Development of the Neural Program

PTB is best known for its role in regulated splicing (Makeyev et al., 2007), which is consistent with our RNA-seq data from HeLa cells (Figure S3F). However, it has been unclear which altered splicing event(s) contributes to the development of the neuronal lineage in PTB-depleted cells. In light of the recent finding that the *REST* gene itself undergoes alternative splicing to produce a truncated, nonfunctional isoform (*REST4*) (Raj et al., 2011), we asked whether this splicing event might be subjected to PTB regulation. We detected some induction of the *REST4* isoform in N2A cells, but not in other cell types we examined (Figure S3G).

During the course of this investigation, we detected induced alternative splicing of two key genes, *LSD1* (a histone lysine demethylase, a component of the REST complex) and *PHF21A* (a component of the histone deacetylase HDAC1 complex) upon PTB knockdown in HeLa and N2A cells (Figures 4A and 4B). This is consistent with multiple PTB binding events around the regulated exon in both cases from our published crosslinking immunoprecipitation (CLIP)-seq data (Xue et al., 2009). Importantly, induced skipping of the alternative exon in *LSD1* has recently been shown to affect neurite morphogenesis/maturation (Zibetti et al., 2010). Although it remains to be determined whether induced *PHF21A* splicing has any functional consequence, these findings suggest that some PTB-regulated splicing events may directly contribute to the neuronal phenotype observed in PTB-downregulated cells.

### PTB Is Involved in the RNA Stability Control of Key Neuronal Genes

Because many PTB-affected genes could not be explained by induced splicing, we searched for other potential mechanisms. PTB has been reported to regulate RNA stability in multiple cases through C/U-rich sequences in the 3' UTR, but the mechanism has remained elusive (Knoch et al., 2004; Kosinski et al., 2003; Pautz et al., 2006; Porter et al., 2008; Tillmar and Welsh, 2002; Woo et al., 2009). By examining the PTB-RNA map (Xue et al., 2009), we noted extensive PTB binding events in the 3' UTR of all of those reported genes (Figure S4A). Globally, PTB binding

on both intronic regions and 3' UTRs are more prevalent than 5' UTRs and exons compared to the RNA-seq signals in these regions (Figure 4C). However, PTB binding alone does not seem to be sufficient to regulate RNA stability, as we showed by using an MS2-based tethering assay (Figures S4B–S4D). We noted that all of those previously mapped PTB-binding sites localize closely with predicted microRNA-targeting sites (Figure S4A), raising an intriguing possibility that PTB may regulate RNA stability via functional interplay with microRNA.

Multiple PTB binding peaks are evident in the 3' UTR of *CoREST* and *HDAC1* (Figure 4D), both of which have been implicated in neurogenesis as key components of the REST complex (Dovey et al., 2010; Hsieh et al., 2004). These mapped PTB-binding sites are coincident with three previously validated targeting sites by miR-124, miR-9, and miR-449 (Baudet et al., 2012; Packer et al., 2008; Selbach et al., 2008). Indeed, PTB knockdown in HeLa cells dramatically reduced the expression of both *CoREST* and *HDAC1* at the protein level and diminished the luciferase activity of the reporters containing the 3' UTR of these genes (Figure 4E). These data strongly suggest that PTB downregulation caused dismantling of multiple components of the REST complex, which likely contribute in a collective fashion to the induction of neuronal-specific genes in non-neuronal cells.

### PTB Regulates RNA Stability in Conjunction with MicroRNA

From this point, we used HeLa cells to understand the mechanism underlying PTB-regulated gene expression mainly because of the experimental manipulability of the cell type, although it is important to emphasize that caution must be taken when extrapolating deduced molecular mechanism from one cell type to another. To determine how extensively PTB is involved in RNA stability control, we performed RNA-seq on mock-depleted and PTB-depleted cells before ( $T_0$ ) or after blocking transcription with Actinomycin D for 4 hr ( $T_4$ ). This allowed us to calculate mRNA decay  $[(T_0 - T_4)/T_0 \times 100\%]$  and determine how such decay might be influenced by PTB for each expressed gene in the human genome. We identified a total of 142 genes that showed significantly increased (red dots in Figure 4F) or decreased (blue dots in Figure 4F) decay ( $p < 0.05$ ) in response to PTB knockdown. Interestingly, *SCP1* is among these genes, which was further confirmed by qRT-PCR (Figure 4G).

We next selected a panel of PTB-bound genes to determine whether these PTB-regulated events were dependent on the microRNA machinery (Figure 4H). We found that many PTB-downregulated genes (blue underlined in Figure 4H) lost the response to PTB knockdown when Ago2 was inactivated. We found no or little effect on several PTB-upregulated genes after Ago2 RNA interference (RNAi) (red underlined in Figure 4H), consistent with the possibility that microRNA no longer acted on these genes in PTB-depleted cells. To determine whether the 3' UTR of PTB-regulated genes might mediate the response to PTB knockdown, we constructed a series of luciferase reporters containing the 3' UTR of these genes, finding that the reporters recaptured PTB-dependent suppression or enhancement (Figure 4I). These data illustrate that PTB is involved in the regulation of RNA stability and/or translational control in

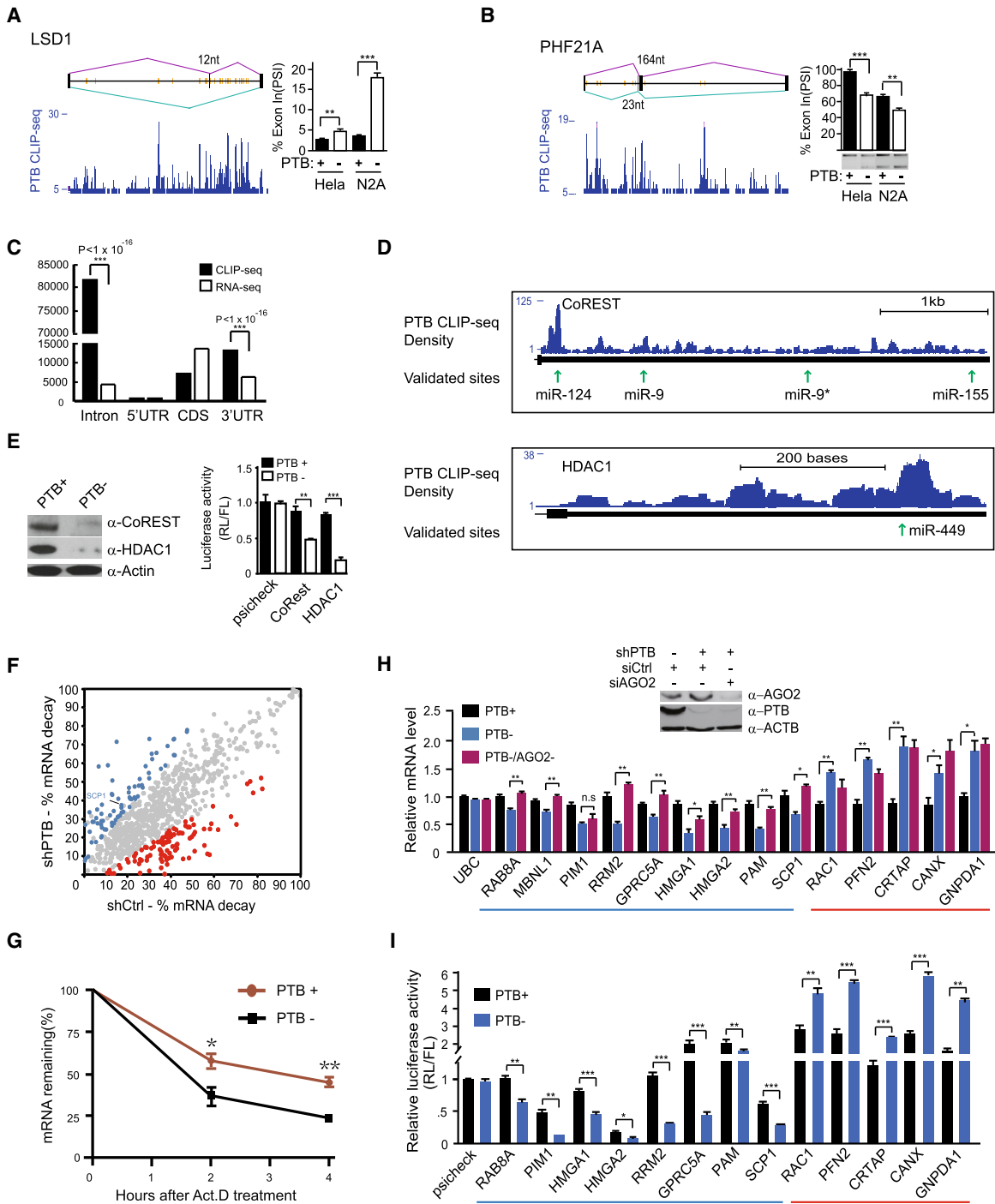


**Figure 4. PTB-Regulated Splicing and RNA Stability**

(A and B) PTB-regulated alternative splicing of *LSD1* and *PHF21A*. The CLIP-seq mapped PTB binding events (blue) are shown along with deduced PTB binding peaks (orange lines) on each gene model. PTB knockdown-induced alternative splicing was determined by qRT-PCR in the case of *LSD1* and by semiquantitative RT-PCR in the case of *PHF21A*.

(C) Relative enrichment of PTB binding in intronic and 3' UTRs. Significant enrichment of PTB binding events is indicated by the p values in each case.

(D) PTB binding on two REST component genes, showing that multiple PTB binding peaks overlap with validated targeting sites by miR-124 and miR-9.

(E) Reduced CoREST and HDAC1 proteins (left) and diminished reporter activities (right) in PTB-depleted HeLa cells.

(F) Genome-wide analysis of PTB-regulated RNA stability. The calculated decay rate was compared in the presence (*shCtrl*-treated) or absence (*shPTB*-treated) of PTB. Genes with increased and decreased decay are highlighted in red and blue, respectively, based on triplicated RNA-seq data ( $p < 0.05$ ).

(G) Accelerated *SCP1* mRNA decay detected by qRT-PCR in PTB-depleted HeLa cells.

(legend continued on next page)

conjunction with the action of microRNA on the 3' UTR of many genes.

### The 3' UTR of *SCP1* Contains Multiple MicroRNA-Targeting Sites

We used *SCP1* as a model to investigate the functional interplay between PTB and microRNA. We compiled PTB and Ago2 CLIP-seq signals (see below in Figure 7) in the 3' UTR of this gene before and after PTB knockdown in order to select relevant regions for functional analysis. We detected one lost and at least six gained Ago2 binding events in the 3' UTR of *SCP1* in response to PTB knockdown (Figure 5A). In the F1 region, for example, we noted three PTB-binding sites that weakly overlap with the mapped Ago2-binding sites before PTB knockdown, and, in response to PTB knockdown, one of these Ago2 CLIP peaks was significantly enhanced, which is near the predicted target site for miR-124. The predicted microRNA-targeting sites in the F1 region are each flanked by a PTB binding consensus motif (Figure 5A, lower panel). Multiple mapped PTB and Ago2 binding events also show various degrees of overlap with the predicted targeting sites for miR-124 and miR-96 in the F2 and F3 regions.

Previous studies showed that forced miR-124 expression could switch the gene expression profile toward that of brain in HeLa cells (Lim et al., 2005). Relevant to the present study, miR-124 has also been shown to be subject to regulation by *SCP1* during neurogenesis in vivo (Visvanathan et al., 2007). Collectively, these observations suggest an important pathway for neuronal differentiation that involves the functional interplay between miR-124, PTB, and *SCP1*/REST.

### PTB Directly Competes with MicroRNA-Targeting on the 3' UTR of *SCP1*

Perturbation experiments confirmed the role of PTB in the regulation of microRNA function. For example, overexpression of miR-96 suppressed *SCP1* expression and PTB knockdown enhanced the effect, whereas miR-96 antagomir showed the opposite response (Figure 5B). A nontargeting miR-339 (labeled as Ctrl miR) served as a negative control. We could recapitulate these effects with a luciferase reporter containing the entire 3' UTR of the *SCP1* gene (Figure S5A). We then analyzed individual segments (F1–F3) in the 3' UTR of *SCP1*, finding that overexpression of either miR-96 or miR-124 could suppress the activity of the reporter containing the F1 fragment (Figure 5C). PTB overexpression antagonized, but PTB knockdown enhanced, the effect of both microRNAs (Figures 5C and 5D). We made a similar observation on the luciferase reporter containing the F2 (Figure S5B) or F3 (Figure S5C) fragment.

To determine the sequence requirement for both microRNA- and PTB-mediated actions, we carried out mutational analysis in the seed region of individual microRNA target sites and on

the nearby PTB-binding sites (Figure 5A). We found that the mutant (GCC to CGG) in the miR-96 seed region no longer responded to the overexpression of this microRNA (Figure 5E). The mutations (double C-to-A) in the nearby PTB-binding site enhanced the effect of the microRNA, even though these mutations impaired miR-96 targeting to some degree, thus causing an increase in the reporter activity in control microRNA-treated cells (Figure 5E). Similarly, the mutations (GCC to CGG) in each of the miR-124-targeting sites attenuated and the double mutation abolished the response to transfected miR-124 (Figure 5F). In comparison, at least one of the mutations in nearby PTB-binding sites (the triple A mutant in the first miR-124-targeting site shown in Figure 5A) enhanced the effect of miR-124 (compare lanes 4 and 12 in Figure 5F). Together, these data demonstrated that PTB directly competes with microRNA on multiple targeting sites in the 3' UTR of the *SCP1* gene.

### PTB Can Also Boost MicroRNA Action on Specific Genes

Our RNA-seq experiments and luciferase-based assays revealed both up- and downregulated genes in response to PTB knockdown. While many upregulated genes likely resulted from derepression, we detected multiple examples of upregulated genes in PTB knockdown cells that appear to depend on their 3' UTRs (Figure 4I). Such effect might be due to PTB-regulated switch of polyadenylation from the distal to proximal site, thereby shortening the 3' UTR in some genes that reduce microRNA-targeting potentials. We tested and ruled out this possibility by measuring RNA-seq tags at the 3' end of each expressed gene in response to PTB knockdown (Figures S5D and S5E).

To understand how PTB knockdown could induce gene expression, we took *GNPDA1* as a model, which was upregulated by PTB via its 3' UTR (Figure 4I). We validated that PTB knockdown enhanced the stability of the endogenous *GNPDA1* transcript (Figure 6A). We noted that the CLIP-seq mapped PTB binding events are coincident with two stretches of C/U-rich sequences on the 3' UTR of the *GNPDA1* gene (Figure 6B). We confirmed high-affinity PTB binding on this element by gel mobility shift (Figure S6A). Importantly, the PTB-binding sites are immediately downstream of the mapped Ago2-binding sites that contain potential targeting sites for several microRNA, including Let-7b, miR-181b, and miR-196a (Figure 6B). As expected, Let-7b overexpression suppressed the expression of the luciferase reporter containing this region, while anti-Let-7b showed the opposite effect (Figure 6C). The reporter activity could be further enhanced by PTB knockdown in HeLa (Figure 6C) and NT2 cells (Figure S6B). We also showed that both anti-Let-7b and anti-miR-181b enhanced *GNPDA1* protein expression in a PTB-dependent manner (Figure 6D). These data demonstrated that microRNAs act more effectively on *GNPDA1* in the presence of PTB.

(H) The effect of knocking down PTB (PTB<sup>-</sup>) or both PTB and Ago2 (PTB<sup>-</sup>/Ago2<sup>-</sup>) on the expression of a panel of genes that show PTB and Ago2 binding events in their 3' UTRs. A gene (UBC) without binding evidence for PTB and Ago2 served as a negative control.

(I) Recapture of PTB-dependent regulation with the 3' UTR of individual genes analyzed in (H). Note that the *MBNL1* gene was not included in this analysis because its 3' UTR is too long to clone.

Data in individual panels are shown as mean ± SD. \*\*p < 0.01; \*\*\*p < 0.001. See also Figure S4.

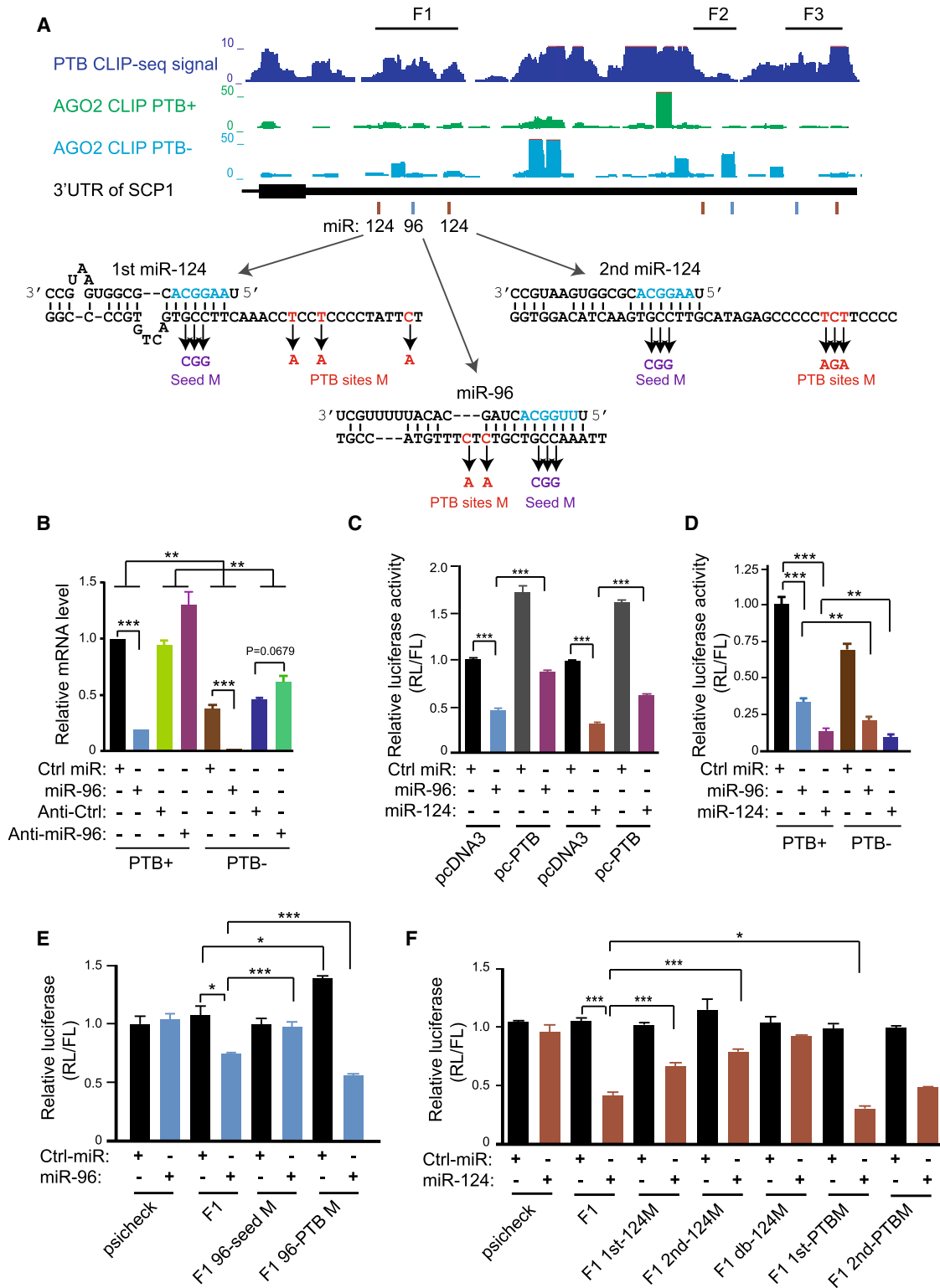


**Figure 5. PTB Competition with MicroRNA Targeting in the 3' UTR of SCP1**

(A) The mapped PTB binding events in the 3' UTR of the *SCP1* gene (top). Above the gene model also show the mapped Ago2 binding density before (green) and after (cyan) PTB knockdown in HeLa cells. Below the gene model indicate multiple predicted microRNA target sites for miR-124 (brown lines) and miR-96 (cyan lines). Arrow-highlighted are deduced base-paired regions between the mRNA and individual microRNAs. Also illustrated are the mutations in the 3' UTR of the *SCP1* gene that correspond to the sequence on the microRNA-targeting sites in the seed region (violet) or on the PTB-binding site (red) in each case.

(legend continued on next page)

### PTB Facilitates MicroRNA Action by Changing Local RNA Secondary Structure

To uncover the mechanism for PTB-dependent enhancement of microRNA action, we determined the secondary structure in the 3' UTR of *GNPDA1* gene using RNase T1 to cut single-stranded RNA after the nucleotide G, and RNase V1 to cleave double-stranded RNA (Figure 6E). This analysis suggests a stem loop between 6U and 33G (Figure 6F), which appears to be undertaking a dynamic switch between the single- and double-stranded states, as evidenced by T1- and V1-cleaved products in the same stem region. In the presence of PTB, we reproducibly detected enhanced single strandness of the stem loop, as indicated by increased T1 cleavage from 10G to 19G (red arrows in Figure 6E) and concurrent decreased V1 cleavage from 19G to 32G (blue arrows in Figure 6E), which were quantified on a modeled RNA structure (boxed in Figure 6F).

We substantiated the increase of single strandness by in-line probing, an approach widely used to detect riboswitches, which measures spontaneous RNA cleavage in solution with strong preference for U-rich residues (Regulski and Breaker, 2008). With increasing amounts of PTB, we found that the entire region gradually opened up, as indicated by enhanced cleavage on nearly all residues from 10G to 33G and the flanking U-rich PTB-binding sites from 34C to 40U (Figure 6G). Thus, PTB appears to induce the exposure of the microRNA target site through binding to multiple pyrimidine-rich regions, including that directly involved in base pairing with microRNA (Figure 6H). In principle, such modulation of RNA secondary structure by PTB or other RNA-binding proteins may enhance or shield microRNA target sites in adjacent regions, thus affecting RNA stability in both directions.

### PTB Globally Regulates MicroRNA-mRNA Interactions in the Human Genome

To assess the global impact of PTB on both positive and negative modulation of microRNA targeting, we conducted CLIP-seq mapping of Ago2 before and after PTB knockdown in HeLa cells. As previously described (Chi et al., 2009), we detected Ago2-RNA crosslinking adducts IPed with anti-Ago2 above the position of the Ago2 protein on SDS-PAGE (Figure 7A). We obtained ~23 million uniquely mapped CLIP-seq tags and identified 4,314 and 4,087 genes that contain at least one Ago2 peak in their 3' UTRs before and after PTB knockdown, respectively. Comparison of these data sets suggests that PTB knockdown generally enhances Ago2 binding in

the human genome (Figure 7B). Ago2 binding events were significantly enriched in the 3' UTR of protein-coding genes in both mock-treated and *shPTB*-treated cells (Figure 7C), especially near the stop codon and the poly(A) site (Figures 7D and 7E).

We next compared the relationship between PTB and Ago2 occupancies in the 3' UTR of protein-coding genes in response to PTB knockdown. The Ago2 binding profiles were similar in the protein-coding side (upstream of the stop codon) on both wild-type (wt) and *shPTB*-treated cells, which provide important internal controls for our comparison. By separately analyzing PTB-bound and -unbound genes, we found that PTB depletion caused a dramatic increase in Ago2 binding in the 3' UTR of PTB-bound targets, but had only a minor effect on PTB-unbound targets (Figures 7D and 7E). These differences are highly statistically significant at the right side of the stop codon and the left side of the Poly(A) sites, as determined by two-tailed Kolmogorov-Smirnov test. This likely represents an underestimate of increased microRNA-targeting events because the transcripts of many PTB-bound genes were downregulated to various degrees in PTB knockdown cells. Global analysis further showed that PTB knockdown generally and significantly enhanced Ago2 binding on and around the mapped PTB-binding sites (Figure 7F). In this analysis, we noted many altered Ago2 binding events around and away from the mapped PTB-binding sites, suggesting that PTB binding may have both local and long-range effects on microRNA targeting.

### PTB-Regulated Ago2 Binding Functionally Correlates to Induced Gene Expression

To determine how such changes in Ago2 binding might be related to altered gene expression, we took a strategy recently used to analyze the interplay between HuR and microRNA (Mukherjee et al., 2011) to segregate expressed genes into five groups based on mapped PTB and Ago2 binding events in their 3' UTRs: (1) -Ago2, -PTB, (2) +Ago2, -PTB, (3) -Ago2, +PTB, (4) +Ago2, +PTB, but no overlap, and (5) +Ago2, +PTB with at least one overlapping binding event within 10 nt. This allowed us to compare gene expression changes in different groups in response to PTB knockdown by plotting genes in each group against induced transcript changes in a cumulative fashion (Figure 7G).

We found no significant differences among groups 1–3, consistent with the lack of PTB and Ago2 actions on these genes. In comparison, relative to genes in group 1 (black line),

(B) The effects on the endogenous *SCP1* mRNA by overexpressed miR-96 and its antagomir before and after PTB knockdown.

(C) Blockage of the effect of overexpressed miR-96 and miR-124 by PTB overexpression on the luciferase reporter containing the F1 fragment from the *SCP1* 3' UTR.

(D) Enhanced effect of overexpressed miR-96 and miR-124 in response to PTB knockdown on the luciferase reporter containing the F1 fragment from the *SCP1* 3' UTR.

(E) The requirement for the seed region in the miR-96 target site to respond to overexpressed miR-96. While the mutations in the PTB-binding site impaired miR-96 targeting (compared lanes 3 and 7), the mutants enhanced the overall effect of miR-96 on the luciferase reporter (compare lanes 3/4 and lanes 7/8).

(F) Contribution of individual miR-124 target sites in the *SCP1* F1 region to microRNA-mediated downregulation of the luciferase activity. The mutations in the seed region of miR-124-targeting sites progressively reduced the response to overexpressed miR-124 (compare lanes 3–10). The mutations in the PTB-binding site near the first miR-124-targeting sites enhanced miR-124-mediated downregulation (compare lanes 4 and 12).

The statistical significance in comparing different groups was determined by paired t test. Data in individual panels are shown as mean  $\pm$  SD. \*\*p < 0.01; \*\*\*p < 0.001. See also Figure S5.

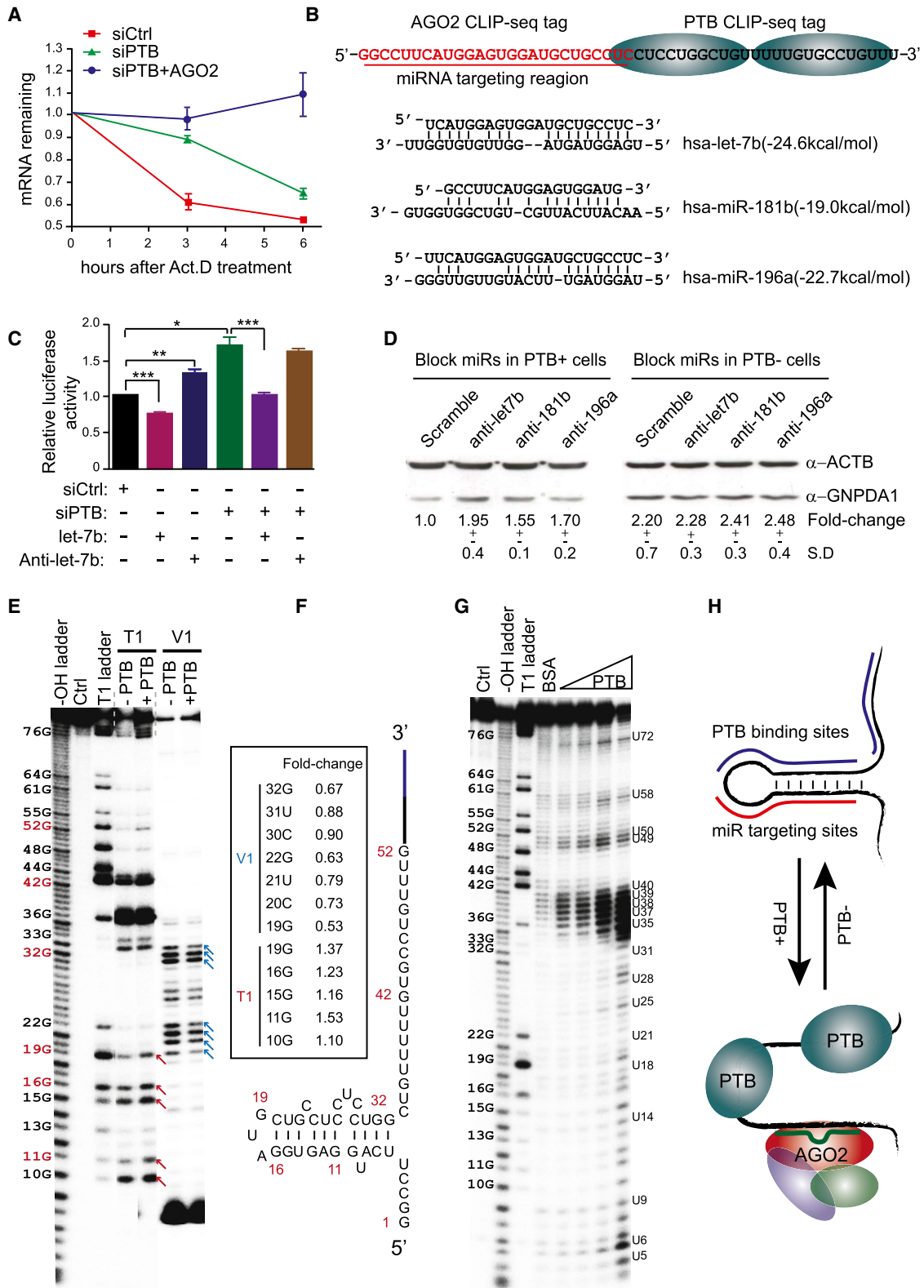


**Figure 6. Enhanced MicroRNA Targeting by Modulating RNA Secondary Structure**

(A) Stabilization of the *GNPDA1* transcript in response to PTB and/or Ago2 knockdown in the presence of the transcription inhibitor Act.D.  
 (B) Potential microRNA-targeting sites near the mapped PTB-binding site in the 3' UTR of *GNPDA1*.

(legend continued on next page)

genes bound by both PTB and Ago2 but with little overlap (group 4, green line) were linked to both repressed (right shift at top) and enhanced gene expression (left shift at bottom), consistent with changes in RNA secondary structure that caused increased or decreased microRNA targeting on different genes (Figure 7G). In contrast, genes bound by both PTB and Ago2 with extensive overlap (group 5, purple line) mainly showed repressed expression (right shift) as a result of enhanced microRNA targeting in the absence of PTB competition (Figure 7G). We obtained similar results in comparing genes in group 2 (Figure S7A) and group 3 (Figure S7B) with those in group 4 and group 5. These results demonstrate a large-scale involvement of PTB in regulated gene expression through its functional interplay with the microRNA machinery, which likely acts in synergy with regulated splicing to propel neurogenesis in mammalian cells.

## DISCUSSION

While the induction of pluripotency with a specific set of stem-cell-specific transcription factors has been well accepted, the field has increasingly recognized the ability of lineage-specific transcription factors to induce differentiated cells to *trans*-differentiate into a different lineage without going back to the fully undifferentiated state. The classic example is MyoD-induced differentiation of fibroblasts to myotubes (Davis et al., 1987), and more recent examples include induced *trans*-differentiation of both embryonic and postnatal fibroblasts into neurons by Ascl1/Mash1 in combination with other enhancing factors (Caiazza et al., 2011; Pang et al., 2011; Qiang et al., 2011; Vierbuchen et al., 2010). Interestingly, this pathway also involves specific microRNAs (Yoo et al., 2011), which are known to act on many critical target genes to induce neuronal differentiation (Li and Jin, 2010). We now report that the reduced expression of a single RNA binding PTB, which occurs during brain development, is able to potently induce differentiation or *trans*-differentiation of diverse cell types into neuronal-like cells or even functional neurons.

Our data highlight the contribution of specific regulated splicing during the induction of neuronal differentiation. More importantly, we discovered a PTB-regulated microRNA program responsible for dismantling of multiple components of REST. We provide further evidence that knockdown of SCP1 or the REST itself is sufficient to trigger *trans*-differentiation of MEFs into neuronal-like cells. The REST complex is well known for its role in suppressing many neuronal genes, including miR-124, in non-neuronal cells, while miR-124 and other neuronal-specific micro-

RNAs target various REST components, including SCP1 and CoREST. This creates a potent regulatory loop (Figure 7H). However, this loop is inefficient, at least in the initial phase of neuronal induction, unless PTB is first downregulated by miR-124. Thus, PTB not only serves as a key target of miR-124, but also functions as a negative regulator for this and other microRNAs to act on their target genes. This represents an interesting regulatory paradigm where the large autoregulatory loop consisting of miR-124 and components of the REST complex is controlled by another feedforward loop that involves PTB.

Strikingly, PTB downregulation induced the expression of all critical transcription factors previously shown to be sufficient to induce *trans*-differentiation of MEFs into functional neurons. Our data provide a mechanism for the induction of these transcription factors because all of these transcription factors appear to be direct REST targets. The puzzle is why genetic ablation of REST or HADC1 impaired self-renewal of neural stem cells, thus preventing unintended neurogenesis in various cellular and animal models (Dovey et al., 2010; Gao et al., 2011; Lee et al., 2002). While the cellular context undoubtedly contributes to such restriction of neurogenesis *in vivo*, it is possible that PTB knockdown may mimic a gradual and sequential switch of a series of events during normal developmental processes by preventing abrupt induction of gene expression that may cause cell death before differentiation. We note that the PTB-regulated RNA program takes place in cells containing induced nPTB and our preliminary results indicate that simultaneous knockdown of PTB and nPTB greatly compromised the development of neuronal morphology. This may indeed represent critical sequential events during normal brain development (Zheng et al., 2012).

Mechanistically, our study joined PTB to a growing list of RNA-binding proteins, including HuR, Dnd1, CRD-BP, and PUM1, that have been implicated in modulating microRNA targeting in mammalian cells (van Kouwenhove et al., 2011). In comparison with previous studies where specific RNA-binding proteins appear to either positively or negatively regulate microRNA targeting, we found that PTB can function in both ways, competing with microRNA targeting on some genes, but promoting microRNA targeting on the others. These two modes of regulation may simultaneously occur on different locations in the same genes, and thus, the net effect of positive and negative regulation may dictate the final functional outcome. These working principles may be generally applicable to many other RNA-binding proteins involved in the regulation of microRNA-mRNA interactions. Our global analysis of Ago2 binding in response to PTB

(C) Overexpressed Let-7b suppressed and antagomir Let-7b enhanced the expression of the luciferase reporter containing the 3' UTR of *GNPDA1* (lanes 1–3). PTB knockdown enhanced the luciferase activity (compared between lanes 1 and 4). Overexpression of Let-7b still suppressed the luciferase activity, but anti-Let-7b no longer showed the effect in PTB knockdown cells.

(D) Antagomir Let-7b, miR-196a, and miR-181b increased *GNPDA1* protein in the presence, but not absence, of PTB in transfected HeLa cells. The protein levels were quantified with the SD shown in the bottom.

(E and F) Mapping the secondary structure in the 3' UTR of *GNPDA1*. Individual G residues were labeled on the left with red indicating several key positions in the deduced secondary structure (E), as modeled (F). Red and blue arrows, respectively, indicate PTB enhanced and suppressed cleavages in the deduced stem-loop region. Quantified fold changes at key positions are indicated in the box inserted in (F).

(G and H) Increased single strandness of RNA in the presence of increasing amounts of PTB detected by in-line probing (G). A proposed model indicates PTB-mediated opening of the stem loop that facilitates microRNA targeting (H).

Data in (A), (C), and (D) are shown as mean  $\pm$  SD. \* $p < 0.05$ ; \*\* $p < 0.01$ ; \*\*\* $p < 0.001$ . See also Figure S6.

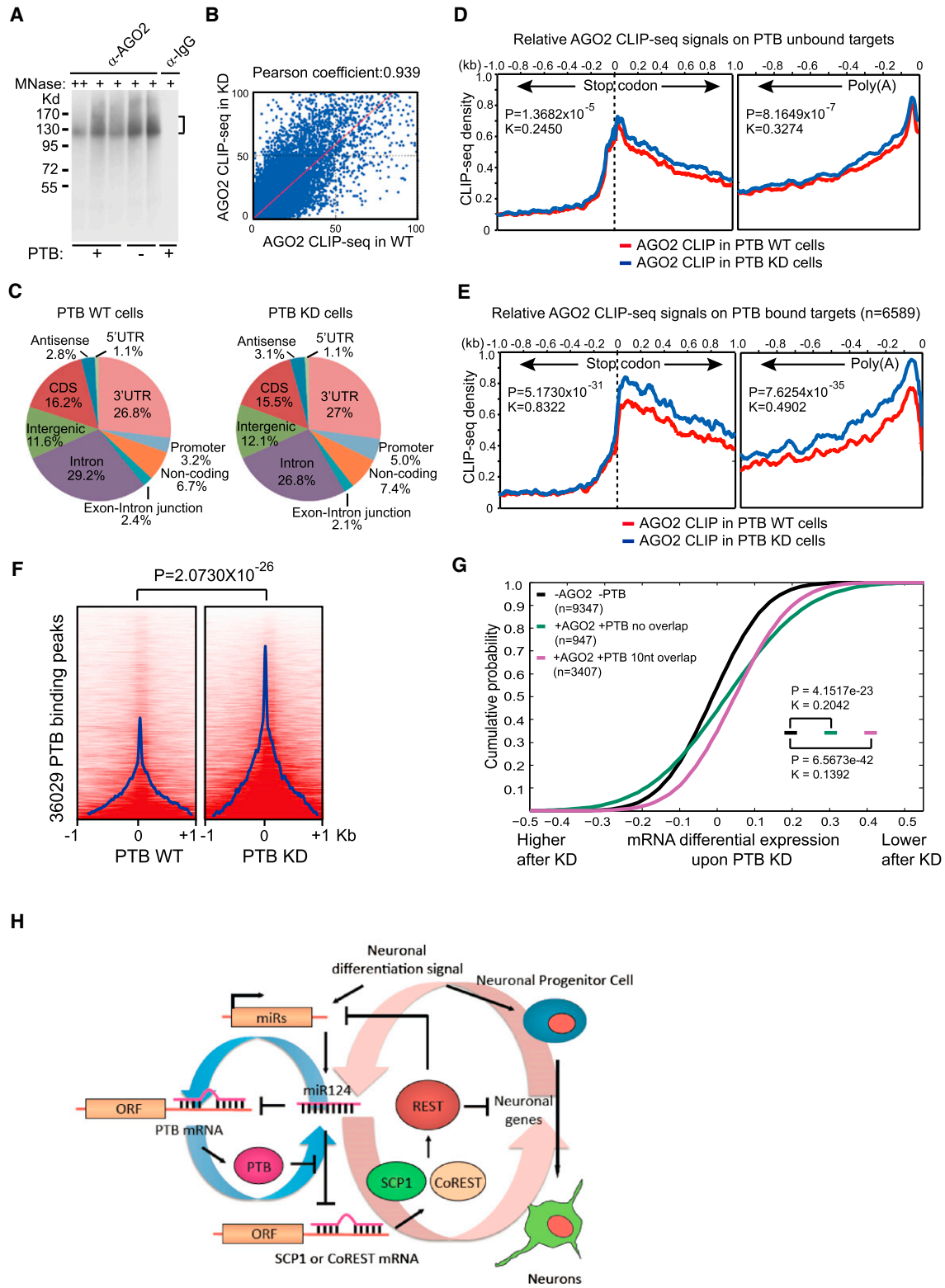


**Figure 7. Global Analysis of Ago2 Binding in Response to PTB Knockdown**

(A) CLIP signals detected with anti-Ago2 before and after PTB knockdown. No signal was detected with IgG control. (B) Comparison between the two Ago2 CLIP-seq data sets in 1 kb windows across the human genome before and after PTB depletion. (C) Genomic distribution of Ago2 binding events before (left) and after (right) PTB knockdown, showing prevalent Ago2 binding in the 3' UTR.

(legend continued on next page)

knockdown also suggests that PTB binding may have some long-range effects on microRNA targeting in addition to local events. This may result from potential PTB-mediated RNA looping, as proposed earlier (Oberstrass et al., 2005), the action of other induced microRNAs, or synergy with other RNA-binding proteins, all of which represent interesting regulatory paradigms to be investigated in future studies.

## EXPERIMENTAL PROCEDURES

### Cell Culture, RNAi, Immunocytochemistry, and Electrophysiological Analysis

Cell culture conditions, treatments with *siRNA* and *shRNA*, and immunocytochemistry are detailed in *Extended Experimental Procedures*. Glial cells were isolated from GFP-transgenic rat brain (Hakamata et al., 2001), and single-cell patch-clamp recordings were performed using an Axopatch 200B amplifier and pClamp 10.0 software (HEKA Elektronik, Lambrecht/Pfalz, Germany), as described in the *Supplemental Information*.

### qRT-PCR, Western Blotting, and Luciferase Assays

qRT-PCR was performed with Fast Start universal SYBR green master mix using gene-specific primers listed in *Table S1*. Luciferase activity was measured 24 hr posttransfection. Western blotting analysis was conducted with various specific antibodies as detailed in *Extended Experimental Procedures*.

### RNA-seq, CLIP-seq, and Probing of RNA Secondary Structure

RNA-seq and CLIP-seq was performed as previously described (Xue et al., 2009). Normalized Ago2 tags are plotted relative to the stop codon at the 3' end of genes as described (Chi et al., 2009). Two-sided Kolmogorov-Smirnov statistics (in the R package, <http://cran.r-project.org/>) was used to determine the significance of the shift in pairwise comparison. RNA footprinting by RNase T1 and V1 was according to the manual from Ambion. The in-line probing assay was as previously described (Regulski and Breaker, 2008), which is also detailed in the *Supplemental Information*.

## ACCESSION NUMBERS

The RNA-seq and CLIP-seq data are available at the Gene Expression Omnibus under the accession number GSE42701.

## SUPPLEMENTAL INFORMATION

Supplemental Information includes *Extended Experimental Procedures*, seven figures, and one table and can be found with this article online at <http://dx.doi.org/10.1016/j.cell.2012.11.045>.

## ACKNOWLEDGMENTS

The authors are grateful to Drs. Gordon Gill, Dongxian Zhang, and Wei Xiong for insightful advice during the course of this investigation and to Drs. Gordon Gill, Amy Pasquinelli, Bruce Hamilton, and Larry Goldstein for critical reading of the manuscript. We thank Drs. Douglas Black, Robert Darnell, Samuel Pfaff, Alysson Muotri, and Geoff Rosenfeld for generous gifts of antibodies and Drs. Zhiping Pang and Marius Wernig for sharing detailed experimental protocols. This work was supported by the China 973 program (2011CB811300,

2012CB910800), the Chinese 111 program grant (B06018), and grants from NIH (GM049369, GM052872, HG004659). H.O. and K.Z. were supported by NIH Director's Transformative RO1 Program (EY021374).

Received: October 26, 2011

Revised: May 16, 2012

Accepted: November 9, 2012

Published: January 10, 2013

## REFERENCES

- Amit, I., Garber, M., Chevrier, N., Leite, A.P., Donner, Y., Eisenhaure, T., Guttman, M., Grenier, J.K., Li, W., Zuk, O., et al. (2009). Unbiased reconstruction of a mammalian transcriptional network mediating pathogen responses. *Science* 326, 257–263.
- Aoki, H., Hara, A., Era, T., Kunisada, T., and Yamada, Y. (2012). Genetic ablation of Rest leads to in vitro-specific derepression of neuronal genes during neurogenesis. *Development* 139, 667–677.
- Auld, K.L., and Silver, P.A. (2006). Transcriptional regulation by the proteasome as a mechanism for cellular protein homeostasis. *Cell Cycle* 5, 1503–1505.
- Ballas, N., Grunseich, C., Lu, D.D., Speh, J.C., and Mandel, G. (2005). REST and its corepressors mediate plasticity of neuronal gene chromatin throughout neurogenesis. *Cell* 121, 645–657.
- Bartel, D.P. (2009). MicroRNAs: target recognition and regulatory functions. *Cell* 136, 215–233.
- Baudet, M.L., Zivraj, K.H., Abreu-Goodger, C., Muldal, A., Armisen, J., Blenkiron, C., Goldstein, L.D., Miska, E.A., and Holt, C.E. (2012). miR-124 acts through CoREST to control onset of Sema3A sensitivity in navigating retinal growth cones. *Nat. Neurosci.* 15, 29–38.
- Boutz, P.L., Stoilov, P., Li, Q., Lin, C.H., Chawla, G., Ostrow, K., Shiue, L., Ares, M., Jr., and Black, D.L. (2007). A post-transcriptional regulatory switch in poly-pyrimidine tract-binding proteins reprograms alternative splicing in developing neurons. *Genes Dev.* 21, 1636–1652.
- Caiazzo, M., Dell'Anno, M.T., Dvoretzskova, E., Lazarevic, D., Taverna, S., Leo, D., Sotnikova, T.D., Menegon, A., Roncaglia, P., Colciago, G., et al. (2011). Direct generation of functional dopaminergic neurons from mouse and human fibroblasts. *Nature* 476, 224–227.
- Carracedo, A., and Pandolfi, P.P. (2008). The PTEN-PI3K pathway: of feedbacks and cross-talks. *Oncogene* 27, 5527–5541.
- Cheng, L.C., Pastrana, E., Tavazoie, M., and Doetsch, F. (2009). miR-124 regulates adult neurogenesis in the subventricular zone stem cell niche. *Nat. Neurosci.* 12, 399–408.
- Chi, S.W., Zang, J.B., Mele, A., and Darnell, R.B. (2009). Argonaute HITS-CLIP decodes microRNA-mRNA interaction maps. *Nature* 460, 479–486.
- Conaco, C., Otto, S., Han, J.J., and Mandel, G. (2006). Reciprocal actions of REST and a microRNA promote neuronal identity. *Proc. Natl. Acad. Sci. USA* 103, 2422–2427.
- Coutinho-Mansfield, G.C., Xue, Y., Zhang, Y., and Fu, X.D. (2007). PTB/nPTB switch: a post-transcriptional mechanism for programming neuronal differentiation. *Genes Dev.* 21, 1573–1577.
- Davis, R.L., Weintraub, H., and Lassar, A.B. (1987). Expression of a single transfected cDNA converts fibroblasts to myoblasts. *Cell* 51, 987–1000.

(D and E) Ago2 binding in the 3' UTR of PTB-unbound (D) and -bound (E) targets before (red) and after (blue) PTB knockdown. Dramatic differences were detected on PTB-bound targets ( $n = 6,589$ ) in (E), which compares to much less responses on a similar number of randomly selected PTB-unbound targets in (D). Statistical significance was determined for the differences on both the stop codon and poly(A) sides by two-tailed Kolmogorov-Smirnov test with both the  $p$  and  $k$  values shown in the inset.

(F) Induction of significant Ago2 binding on and near the PTB-binding sites. The  $p$  value for the differences is indicated on the top.

(G) Functional correlation between PTB/microRNA interplay and gene expression. Genes with induced and repressed expression are plotted in a cumulative fashion. Statistical significance was determined by Kolmogorov-Smirnov test.

(H) Model for the PTB-regulated miR124-REST loop. See also *Figure S7*.

- Dovey, O.M., Foster, C.T., and Cowley, S.M. (2010). Histone deacetylase 1 (HDAC1), but not HDAC2, controls embryonic stem cell differentiation. *Proc. Natl. Acad. Sci. USA* *107*, 8242–8247.
- Gao, Z., Ure, K., Ding, P., Nashaat, M., Yuan, L., Ma, J., Hammer, R.E., and Hsieh, J. (2011). The master negative regulator REST/NRSF controls adult neurogenesis by restraining the neurogenic program in quiescent stem cells. *J. Neurosci.* *31*, 9772–9786.
- Hakamata, Y., Tahara, K., Uchida, H., Sakuma, Y., Nakamura, M., Kume, A., Murakami, T., Takahashi, M., Takahashi, R., Hirabayashi, M., et al. (2001). Green fluorescent protein-transgenic rat: a tool for organ transplantation research. *Biochem. Biophys. Res. Commun.* *286*, 779–785.
- He, X., Pool, M., Darcy, K.M., Lim, S.B., Auersperg, N., Coon, J.S., and Beck, W.T. (2007). Knockdown of polypyrimidine tract-binding protein suppresses ovarian tumor cell growth and invasiveness in vitro. *Oncogene* *26*, 4961–4968.
- Hsieh, J., Nakashima, K., Kuwabara, T., Mejia, E., and Gage, F.H. (2004). Histone deacetylase inhibition-mediated neuronal differentiation of multipotent adult neural progenitor cells. *Proc. Natl. Acad. Sci. USA* *101*, 16659–16664.
- Johnson, D.S., Mortazavi, A., Myers, R.M., and Wold, B. (2007). Genome-wide mapping of in vivo protein-DNA interactions. *Science* *316*, 1497–1502.
- Kim, J., Efe, J.A., Zhu, S., Talantova, M., Yuan, X., Wang, S., Lipton, S.A., Zhang, K., and Ding, S. (2011). Direct reprogramming of mouse fibroblasts to neural progenitors. *Proc. Natl. Acad. Sci. USA* *108*, 7838–7843.
- Knoch, K.P., Bergert, H., Borgonovo, B., Saeger, H.D., Altkrüger, A., Verkade, P., and Solimena, M. (2004). Polypyrimidine tract-binding protein promotes insulin secretory granule biogenesis. *Nat. Cell Biol.* *6*, 207–214.
- Kosinski, P.A., Laughlin, J., Singh, K., and Covey, L.R. (2003). A complex containing polypyrimidine tract-binding protein is involved in regulating the stability of CD40 ligand (CD154) mRNA. *J. Immunol.* *170*, 979–988.
- Lareau, L.F., Inada, M., Green, R.E., Wengrod, J.C., and Brenner, S.E. (2007). Unproductive splicing of SR genes associated with highly conserved and ultra-conserved DNA elements. *Nature* *446*, 926–929.
- Lee, T.I., Rinaldi, N.J., Robert, F., Odom, D.T., Bar-Joseph, Z., Gerber, G.K., Hannett, N.M., Harbison, C.T., Thompson, C.M., Simon, I., et al. (2002). Transcriptional regulatory networks in *Saccharomyces cerevisiae*. *Science* *298*, 799–804.
- Leung, A.K., and Sharp, P.A. (2010). MicroRNA functions in stress responses. *Mol. Cell* *40*, 205–215.
- Li, X., and Jin, P. (2010). Roles of small regulatory RNAs in determining neuronal identity. *Nat. Rev. Neurosci.* *11*, 329–338.
- Lim, L.P., Lau, N.C., Garrett-Engle, P., Grimson, A., Schelter, J.M., Castle, J., Bartel, D.P., Linsley, P.S., and Johnson, J.M. (2005). Microarray analysis shows that some microRNAs downregulate large numbers of target mRNAs. *Nature* *433*, 769–773.
- Makeyev, E.V., Zhang, J., Carrasco, M.A., and Maniatis, T. (2007). The MicroRNA miR-124 promotes neuronal differentiation by triggering brain-specific alternative pre-mRNA splicing. *Mol. Cell* *27*, 435–448.
- Mukherjee, N., Corcoran, D.L., Nusbaum, J.D., Reid, D.W., Georgiev, S., Hafner, M., Ascano, M., Jr., Tuschi, T., Ohler, U., and Keene, J.D. (2011). Integrative regulatory mapping indicates that the RNA-binding protein HuR couples pre-mRNA processing and mRNA stability. *Mol. Cell* *43*, 327–339.
- Nowak, L., Bregestovski, P., Ascher, P., Herbet, A., and Prochiantz, A. (1984). Magnesium gates glutamate-activated channels in mouse central neurones. *Nature* *307*, 462–465.
- Oberstrass, F.C., Auweter, S.D., Erat, M., Hargous, Y., Henning, A., Wenter, P., Reymond, L., Amir-Ahmady, B., Pitsch, S., Black, D.L., and Allain, F.H. (2005). Structure of PTB bound to RNA: specific binding and implications for splicing regulation. *Science* *309*, 2054–2057.
- Packer, A.N., Xing, Y., Harper, S.Q., Jones, L., and Davidson, B.L. (2008). The bifunctional microRNA miR-9/miR-9\* regulates REST and CoREST and is downregulated in Huntington's disease. *J. Neurosci.* *28*, 14341–14346.
- Pang, Z.P., Yang, N., Vierbuchen, T., Ostermeier, A., Fuentes, D.R., Yang, T.Q., Citri, A., Sebastiano, V., Marro, S., Südhof, T.C., and Wernig, M. (2011). Induction of human neuronal cells by defined transcription factors. *Nature* *476*, 220–223.
- Pautz, A., Linker, K., Hubrich, T., Korhonen, R., Altenhöfer, S., and Kleinert, H. (2006). The polypyrimidine tract-binding protein (PTB) is involved in the post-transcriptional regulation of human inducible nitric oxide synthase expression. *J. Biol. Chem.* *281*, 32294–32302.
- Porter, J.F., Vavassori, S., and Covey, L.R. (2008). A polypyrimidine tract-binding protein-dependent pathway of mRNA stability initiates with CpG activation of primary B cells. *J. Immunol.* *181*, 3336–3345.
- Qiang, L., Fujita, R., Yamashita, T., Angulo, S., Rhinn, H., Rhee, D., Doege, C., Chau, L., Aubry, L., Vanti, W.B., et al. (2011). Directed conversion of Alzheimer's disease patient skin fibroblasts into functional neurons. *Cell* *146*, 359–371.
- Raj, B., O'Hanlon, D., Vessey, J.P., Pan, Q., Ray, D., Buckley, N.J., Miller, F.D., and Blencowe, B.J. (2011). Cross-regulation between an alternative splicing activator and a transcription repressor controls neurogenesis. *Mol. Cell* *43*, 843–850.
- Regulski, E.E., and Breaker, R.R. (2008). In-line probing analysis of riboswitches. *Methods Mol. Biol.* *419*, 53–67.
- Selbach, M., Schwanhäusser, B., Thierfelder, N., Fang, Z., Khanin, R., and Rajewsky, N. (2008). Widespread changes in protein synthesis induced by microRNAs. *Nature* *455*, 58–63.
- Tillmar, L., and Welsh, N. (2002). Hypoxia may increase rat insulin mRNA levels by promoting binding of the polypyrimidine tract-binding protein (PTB) to the pyrimidine-rich insulin mRNA 3'-untranslated region. *Mol. Med.* *8*, 263–272.
- van Kouwenhove, M., Kedde, M., and Agami, R. (2011). MicroRNA regulation by RNA-binding proteins and its implications for cancer. *Nat. Rev. Cancer* *11*, 644–656.
- Vierbuchen, T., Ostermeier, A., Pang, Z.P., Kokubu, Y., Südhof, T.C., and Wernig, M. (2010). Direct conversion of fibroblasts to functional neurons by defined factors. *Nature* *463*, 1035–1041.
- Visvanathan, J., Lee, S., Lee, B., Lee, J.W., and Lee, S.K. (2007). The microRNA miR-124 antagonizes the anti-neural REST/SCP1 pathway during embryonic CNS development. *Genes Dev.* *21*, 744–749.
- Watanabe, Y., Kameoka, S., Gopalakrishnan, V., Aldape, K.D., Pan, Z.Z., Lang, F.F., and Majumder, S. (2004). Conversion of myoblasts to physiologically active neuronal phenotype. *Genes Dev.* *18*, 889–900.
- Woo, K.C., Kim, T.D., Lee, K.H., Kim, D.Y., Kim, W., Lee, K.Y., and Kim, K.T. (2009). Mouse period 2 mRNA circadian oscillation is modulated by PTB-mediated rhythmic mRNA degradation. *Nucleic Acids Res.* *37*, 26–37.
- Xue, Y., Zhou, Y., Wu, T., Zhu, T., Ji, X., Kwon, Y.S., Zhang, C., Yeo, G., Black, D.L., Sun, H., et al. (2009). Genome-wide analysis of PTB-RNA interactions reveals a strategy used by the general splicing repressor to modulate exon inclusion or skipping. *Mol. Cell* *36*, 996–1006.
- Yang, N., Ng, Y.H., Pang, Z.P., Südhof, T.C., and Wernig, M. (2011). Induced neuronal cells: how to make and define a neuron. *Cell Stem Cell* *9*, 517–525.
- Yeo, M., Lee, S.K., Lee, B., Ruiz, E.C., Pfaff, S.L., and Gill, G.N. (2005). Small CTD phosphatases function in silencing neuronal gene expression. *Science* *307*, 596–600.
- Yoo, A.S., Sun, A.X., Li, L., Shcheglovitov, A., Portmann, T., Li, Y., Lee-Messer, C., Dolmetsch, R.E., Tsien, R.W., and Crabtree, G.R. (2011). MicroRNA-mediated conversion of human fibroblasts to neurons. *Nature* *476*, 228–231.
- Zernicka-Goetz, M., Morris, S.A., and Bruce, A.W. (2009). Making a firm decision: multifaceted regulation of cell fate in the early mouse embryo. *Nat. Rev. Genet.* *10*, 467–477.
- Zheng, S., Gray, E.E., Chawla, G., Porse, B.T., O'Dell, T.J., and Black, D.L. (2012). PSD-95 is post-transcriptionally repressed during early neural development by PTBP1 and PTBP2. *Nat. Neurosci.* *15*, 381–388.
- Zibetti, C., Adamo, A., Binda, C., Forneris, F., Toffolo, E., Verpelli, C., Ginelli, E., Mattevi, A., Sala, C., and Battaglioli, E. (2010). Alternative splicing of the histone demethylase LSD1/KDM1 contributes to the modulation of neurite morphogenesis in the mammalian nervous system. *J. Neurosci.* *30*, 2521–2532.